Seasonally Transported Aerosol Layers over Southeast Atlantic are Closer to Underlying Clouds than Previously Reported

Chamara Rajapakshe[1], Zhibo Zhang[1,2*]
John E. Yorks[3], Hongbin Yu[3], Qian Tan[4], Kerry Meyer[3], Steven Platnick[3] David M. Winker[5]

1. Physics Department, UMBC, Baltimore, MD
2. Joint Center for Earth System Technology, UMBC, Baltimore, MD
3. NASA Goddard Space Flight Center, Greenbelt, MD
4. NASA Ames Research Center, Moffett Field, CA
5. NASA Langley Research Center, Hampton, VA

*Corresponding Author:
Dr. Zhibo Zhang
Email: Zhibo.zhang@umbc.edu
Phone: (410) 455-6315

For publication in *Geophysical Research Letters*

Abstract:
From June to October, low-level clouds in the Southeast (SE) Atlantic often underlie seasonal aerosol layers transported from African continent. Previously, the Cloud-Aerosol Lidar and Infrared Pathfinder Satellite Observation (CALIPSO) 532 nm lidar observations have been used to estimate the relative vertical location of the above-cloud aerosols (ACA) to the underlying clouds. Here, we show new observations from NASA's Cloud-Aerosol Transport System (CATS) lidar. Two seasons of CATS 1064 nm observations reveal that the bottom of the ACA layer is much lower than previously estimated based on CALIPSO 532nm observations. For about 60% of CATS nighttime ACA scenes, the aerosol layer base is within 360 m distance to the top of the underlying cloud. Our results are important for future studies of the microphysical indirect and semi-direct effects of ACA in the SE Atlantic region.

1. Introduction

Every year from about June to October over the southeast (SE) Atlantic, the prevailing easterly winds in the free troposphere often transport the smoke and pollution aerosols from the African continent to the west, over the ocean where extensive marine boundary layer (MBL) clouds persist for most of the year [*Adebiyi and Zuidema*, 2016]. This leads to a near-persistent seasonal biomass burning aerosol layer over MBL clouds in SE Atlantic [*Devasthale and Thomas*, 2011; *Zhang et al.*, 2016].

As summarized in Yu and Zhang [2013] instruments onboard NASA's A-train satellite constellation provide valuable observations of the aerosol layer and underlying clouds. In particular, the lidar on the space-borne mission CALIPSO provides unique observations of the vertical distribution of the aerosol layer that have been widely used to characterize the aerosol layer above cloud over SE Atlantic [*Chand et al.*, 2008; *Yu et al.*, 2010; *Devasthale and Thomas*, 2011; *Meyer et al.*, 2013] and assess its impacts on the radiation budget [*Chand et al.*, 2009; *Zhang et al.*, 2016].

The seasonally transported SE Atlantic aerosol layer can influence the regional radiative energy budget through the direct radiative effect (DRE) [*Chand et al.*, 2009; *Zhang et al.*, 2016]. The absorption by aerosol layer can also influence the thermodynamical structure of lower atmosphere and in turn change cloud field, which is known as the semi-direct effect [*Johnson et al.*, 2004; *Wilcox*, 2010; *Sakaeda et al.*, 2011; *Wilcox*, 2012]. The sign and magnitude of the semi-direct effect are strongly dependent on the vertical distribution of aerosol with respect to the underlying clouds [*Johnson et al.*, 2004]. In addition to DRE and semi-direct effect, the aerosol particles could be entrained into the clouds and activated as cloud condensation nuclei, giving rise to the so-called aerosol indirect effects [*Costantino and Bréon*, 2010; 2013; *Painemal et al.*, 2015]. Intuitively, the closer the bottom of the aerosol layer gets to the top of underlying cloud, the more likely the aerosol particles are entrained into the cloud. Previous studies have used the 532 nm observations from the CALIPSO lidar to estimate the distance from the aerosol layer bottom to the cloud top (referred to hereafter as AB2CT distance for short). Costantino & Bréon [2010] show that 84% of the time the AB2CT distance in SE Atlantic is larger than 250m. Devasthale and Thomas [2011] found that in 0º to 30ºS region, 90-95% of above-cloud-aerosol cases has an AB2CT distance greater than 100m. Yu et al. [2010] derived the average AB2CT of 1700 m over a two-year period in SE Atlantic. These analyses based on CALIOP 532 nm observations seem to indicate that the seasonal aerosol layer in SE Atlantic is well separated from the underlying clouds and thus the aerosol indirect effects may be secondary in comparison to the aerosol direct and semi-direct effects (e.g., [*Sakaeda et al.*, 2011]).

It is known that the CALIOP 532 nm based layer detection often misses the lowest boundary of a thick aerosol layer, thereby biasing the bottom of the aerosol layer too high. This may be especially problematic for daytime observations [*Meyer et al.*, 2013]. Recently, several novel remote sensing techniques have been developed to retrieve the AOD (Aerosol Optical Depth) of above-cloud absorbing aerosol layers from passive sensors (e.g. [*Waquet et al.*, 2009; *Torres et al.*, 2011; *Meyer et al.*, 2015]). In addition, an alternative lidar method has been developed for CALIOP, utilizing signals from the underlying cloud instead of the attenuated backscatter profile [*Hu et al.*, 2007; *Liu et al.*, 2015]. When compared with the retrievals from passive sensors and the alternative CALIOP algorithm, the operational 532nm CALIOP AOD retrievals are systematically biased low by 26% on average [*Liu et al.*, 2015], and can be up to a factor of 5 lower [*Jethva et al.*, 2014]. A likely explanation for this bias is that the strong aerosol attenuation at 532 nm by the upper portion of the aerosol layer together with the small backscatter cross section of the aerosol particles, substantially weakens the attenuated backscatter signal from the lower part of the aerosol layer to a level under the detection threshold of CALIOP [*Kacenelenbogen et al.*, 2011; *Torres et al.*, 2013; *Jethva et al.*, 2014; *Liu et al.*, 2015]. This laser attenuation issue leads to an overestimation of the aerosol layer bottom height (too high), an underestimation of the physical thickness of the aerosol layer (too thin), and thereby an underestimation of AOD (too small).

In this study, we seek to shed new light on the vertical distribution of the SE Atlantic absorbing aerosol layer with respect to the underlying clouds using observations from NASA's CATS mission. Because of instrument and algorithm differences, CATS ACA retrieval suffers much less from the laser saturation-induced bias than CALIOP 532nm algorithm. We do a comparative analysis of CATS and CALIOP retrievals in the SE Atlantic region for two recent biomass burning seasons (2015 and 2016). As shown in the letter, the CATS 1064nm observations suggest that bottom of the ACA layer is much lower, and therefore closer to underlying cloud top, than previously estimated based on CALIOP 532nm observations. Our results are important for future studies of the microphysical indirect, as well as the semi-direct, effects of ACA on underlying clouds.

2. Data

The occurrence frequency of above-cloud-aerosol in the SE Atlantic (20W to 20E; 30S to 10N) is highest during July-to-October (JASO) with the peak during August-September [*Zhang et al.*, 2016]. In this study, we focus on the two biomass burning seasons (JASO) of 2015 and 2016 so that we can directly compare CALIPSO and CATS (Figure 1).

2.1. CALIOP

The lidar instrument onboard the CALIPSO mission, which has an orbital height of ~700 km, is the Cloud-Aerosol Lidar with Orthogonal Polarization (CALIOP). CALIOP directly measures the range-resolved total (particulate plus molecular) attenuated backscatter signal at two wavelengths, 532nm and 1064nm, using analog detection. In addition to the total attenuated backscatter, CALIOP also measures two orthogonal polarized components of the 532nm-backscatter signal [*Winker et al.*, 2009]. The accuracy of the CALIOP Level-2 (L2) data products (aerosol type, particulate backscatter and extinction coefficient, optical depth) is dependent on the accurate detection of cloud and aerosol layers.

Uniform cloud and aerosol layer detection and cloud-aerosol discrimination (CAD) techniques are challenging due to the complexity of atmospheric scenes encountered. The current version CALIOP selective, iterated boundary location (SIBYL) algorithm uses the 532nm total attenuated backscattered signals to determine boundaries of cloud and aerosol layers, with a typical vertical resolution of 30 m [*Vaughan et al.*, 2009]. The SIBYL scheme detects atmospheric features by iteratively comparing horizontally averaged CALIOP 532 nm total attenuated backscatter profiles at multiple horizontal resolutions. The CALIOP CAD algorithm is a multidimensional probability distribution function (PDF) technique [*Liu et al.*, 2004; 2009] based on statistical differences of several cloud and aerosol properties (e.g., layer-integrated 532nm attenuated backscatter, layer-integrated backscatter color ratio, etc.). Previous studies have shown the SIBYL and CAD algorithms perform well for cirrus clouds and several aerosol types [*McGill et al.*, 2007; *Yorks et al.*, 2011; *Burton et al.*, 2013].

2.2. CATS

CATS is an elastic backscatter lidar employing photon counting detection and two high-repetition rate lasers that operate at 532 and 1064nm [*McGill et al.*, 2015] that has been operating on the ISS since February 2015. The ISS orbit, which is at an altitude of ~415 km and a 51-degree inclination, allows CATS to observe locations at different local times each overpass (~60 days to complete full diurnal cycle) with roughly a three-day repeat cycle.

The CATS layer detection algorithm is a threshold-based layer detection method that is nearly identical to the CALIOP-SIBYL technique with four distinct differences, namely the use of 60 m vertical resolution, a single horizontal spatial resolution (5km), the use of the 1064nm wavelength rather than 532nm, and a technique to identify clouds embedded within aerosol layers [*Yorks et al.*, 2015]. The CATS L2 Operational (L2O) CAD algorithm is a multidimensional PDF technique like the CALIOP one [Yorks et al. 2015], but uses the layer-integrated attenuated backscatter at 1064 nm and other variables such as layer mid-temperature and layer thickness instead of the layer-integrated backscatter color ratio due to the unreliable 532 nm data in Mode 7.2. The use of a single horizontal spatial resolution in the CATS algorithm misses optically thin cirrus clouds and aerosols during the daytime in the CATS L2O Version 1-05 data products, though it performs well during nighttime observations. Future versions of CATS L2O data products will include layer detection at 60 km, but since Version 1-05 is used in this study, CATS daytime data was excluded.

For above-cloud aerosol (ACA), the more relevant difference between the algorithms is the preferred wavelength for atmospheric layer detection. The current CALIOP-SIBYL primarily uses 532 nm because it has higher signal-to-noise ratios (SNR) and lower minimum detectable backscatter (MDB,weakest aerosol backscatter coefficient that can be detected) than the CALIOP 1064 nm data resulting in more accurate uniform cloud and aerosol layer detection [*Vaughan et al.*, 2009]. The CATS layer detection algorithm uses the 1064 nm attenuated scattering ratio because the CATS 532 nm data in Mode 7.2 is extremely noisy and the 1064 nm MDB is orders of magnitude lower [*Yorks et al.*, 2016]. For ACA detection specifically, the 1064 nm wavelength is preferred over the 532 nm wavelength for layer detection. The aerosol signal at 1064 nm has sixteen times less molecular contamination compared to 532 nm. As discussed in Section 1, the 532 nm backscatter signal may be insensitive to the entire vertical extent of absorbing aerosol layers. Because aerosol extinction is usually smaller at 1064 nm than 532 nm, and the CATS 1064nm backscatter signal is very robust, the vertical extent of absorbing aerosol layers is fully captured from CATS 1064 nm backscatter profiles. It is worth mentioning that the current CATS operational algorithm uses AB2CT<360 m as the threshold to detect the clouds embedded within aerosol layers (CEAL) [Yorks et al. 2017]. When AB2CT<360, the ACA and the cloud below is merged and identified a CEAL case.

The detectability of the aerosol layer base using 532 and 1064 nm is demonstrated in Figure 1. CATS and CALIPSO passed over the same ACA layer over the SE Atlantic on 06 August 2016, although the differing orbits of the ISS and CALIPSO mean that the two curtains do not align exactly. There is a 0.1-1.0 km gap between cloud top and aerosol base in the attenuated total backscatter and vertical feature mask based on CALIOP 532 nm data. In contrast, CATS 1064 nm observation finds the aerosol plume to extend all the way to the cloud top, which is also confirmed by the CALIOP 1064nm attenuated backscatter observation. The example clearly demonstrates the advantage of 1064nm over 532 nm-based layer detection technique for identifying the bottom of thick smoke layers. Although CALIOP also has the 1064 nm observation, it has not yet been utilized in the current operational algorithm. Note that the differences between CALIOP and CATS observations shown below are mainly due to the use of different wavelength (i.e., 532nm vs. 1064nm) for layer detection. At the moment of writing, the CALIPSO operational product team is planning to make more use of the 1064nm observations in their operational layer detection algorithm, which could significantly improve its retrievals for thick aerosol layers like the example in Figure 1.

3. Results

We have used the following criteria to identify ACA columns in both CALIOP and CATS layer products: (1) the cloud layer product identifies liquid phase cloud at the top layer of the profile; (2) the aerosol layer product identifies at least one layer of aerosol in the profile; (3) the base height of at least one aerosol layer is higher than the top of the highest cloud layer. In the SE Atlantic region, most ACA cases are simple, with only one aerosol layer on top of single-layer MBL clouds. After the identification of ACA columns, we compute the AB2CT by calculating the difference between the minimum aerosol base height which is greater than maximum cloud top height and the maximum cloud top height. For CALIOP, we derived the ACA and cloud statistics for both daytime and nighttime conditions (though daytime and nighttime statistics are computed separately). The CATS results are only for nighttime since its aerosol retrieval does not perform well during daytime at the fixed 5 km horizontal resolution as discussed above.

Figure 2 (first row) shows the multi-year (2015-2016) SE Atlantic JASO Cloud Fraction (CF), defined as $CF = N_{cloudy}/N_{total}$ in $2^o \times 2^o$ grid boxes where N_{cloudy} is the number of cloudy columns and N_{total} is the number of total columns. Because we are interested in aerosol above low-level MBL clouds, ACA frequency (ACA_F) is shown in the second row of Figure 2 is defined as $ACA\_F = N_{ACA}/N_{cloudy}$ where N_{ACA} is the number of ACA columns. Among the three datasets, CATS nighttime observations identify the highest ACA occurrence frequency, with domain averaged ACA_F around 0.24. CALIOP daytime observations have the lowest ACA occurrence frequency, with domain averaged ACA_F only around 0.17. The CALIOP nighttime observations are comparable to the CATS nighttime observations (domain average ACA_F ~ 0.23). Some differences between the three datasets may have physical explanations. For example, CALIOP observes a larger CF during nighttime than during daytime, which is likely a result of the strong cloud diurnal cycle in the SE Atlantic region [*Min and Zhang*, 2014]. The other differences may stem from algorithm and instrument differences. For example, the lower ACA_F using daytime CALIOP might be an artifact due to the impact of background solar noise on the lidar retrieval [*Liu et al.*, 2015].

Overall, the results in Figure 2 suggest that, despite some minor differences, CALIOP and CATS observe similar geographical patterns of ACA in the SE Atlantic. We now focus on the vertical distribution of aerosol and cloud from the two instruments. Figure 3 shows the two-year (2015-2016) mean aerosol layer base height (top row), cloud layer top height (middle row) and AB2CT distance (bottom row) of ACA over the SE Atlantic region during JASO from CALIOP and CATS. While the magnitudes differ, cloud top heights from all three datasets show a similar pattern, lowest off the coast of Namibia (near 20S and 10E) and gradually increasing along the northwest direction to about 2km around 5S and 15W. In contrast to the similarity of cloud top height, the mean ACA base height from the three datasets show significant differences. ACA base height from daytime CALIOP observations is much higher than nighttime CALIOP, which is in turn higher than nighttime CATS. As a result, the AB2CT distance from nighttime CATS is below 500m in most of the SE Atlantic region, suggesting that the aerosol layer extends close to the cloud top. On the other hand, a clear separation between aerosol base and cloud top during both daytime and nighttime is implied by the CALIOP data, a likely result of the abovementioned CALIOP ACA layer detection issues.

We analyzed the AB2CT distances from the three observations further in Figure 4. Here, we show the Cumulative Density Function (CDF) of the AB2CT distance for the sampling-masked ACA cases of Fig. 3. According to CATS nighttime 1064 nm observations (red curve), about 60% of ACA cases are identified as CEAL (i.e., AB2CT<360m), in contrast to only 15% and 6% occurrence of such cases in CALIOP 532nm nighttime (blue curve) and daytime (green curve) observations, respectively. Moreover, 82% and 64% of ACA cases have AB2CT>1 km according to the daytime and nighttime CALIOP 532nm observations, respectively, in contrast to 22% according to CATS observations.

Figure 5 shows meridionally-averaged daytime (a) and nighttime CALIOP (b) 532nm, and nighttime CATS 1064nm (c) observations of ACA top (dashed red line) and bottom (solid red line) height, cloud top height (blue line), and the fraction of ACA cases with AB2CT<360m (black line). Also shown are one standard deviation variability for ACA top (red error bars), ACA base (light red shades) and cloud top (light blue shades). All three observations show nearly the same top of aerosol layer, just below 4km. The cloud top heights are also similar in all three observations, rising from 1km near the coast westward to about 1.5-2.0 km at 19W. Daytime CALIOP observes slightly higher cloud top height (domain average 1.39km) compared to nighttime (domain average 1.33km). Among all the observations, the CATS detects the highest cloud top height (domain average 1.60km) among all three data sets. In contrast to aerosol top and cloud top heights, ACA base heights are substantially different among the three data sets. The CALIOP nighttime product (Figure 5b) gives domain-averaged ACA base height at 2.63km; daytime CALPSO retrievals (Figure 5a) are even higher. Nighttime CATS 1064 nm (Figure 5c), however, observes a significantly lower ACA domain-averaged base height around 2km.

Even after considering one standard deviation variability, there is still a clear separation between the ACA base and cloud top in both the daytime (Figure 5a) and nighttime (Figure 5b) CALIOP retrievals, confirmed by the small values of AB2CT<360m throughout the domain. With CATS (Figure 5c), however, there is clear evidence that the ACA base and cloud top are in much closer proximity than is implied by CALIOP 532nm observation, as the AB2CT<360m is mostly around 60%.

4. Summary and Discussion

The microphysical indirect effects of the seasonal transported aerosols in the SE Atlantic are often overlooked in the literature. This is partly because CALIOP's 532nm-based operational layer detection algorithm often detects the aerosol layer bottom too high and thereby suggests that the above-cloud aerosol layer is well separated from the underlying clouds. The newly launched CATS mission provides a new dataset of the vertical distribution of aerosol and clouds. Several instrument and algorithm advantages of CATS, chiefly among which is the primary use of 1064 nm for layer detection, allows it to better identify the full vertical extend of the SE Atlantic ACA layer than CALIOP 532nm product. We have compared the current CATS and CALIPSO products during JASO of 2015 and 2016 over the SE Atlantic. The CF, ACA_F and cloud top geographical patterns from the two instruments agree well. However, CATS 1064nm observes the ACA layer bottom height much lower and much closer to the underlying cloud top than CALIOP 532nm does. According to CATS, about 60% of the ACA cases have an AB2CT<360m, in contrast to the 15% and 6% based on CALIOP nighttime and daytime 532nm observations, respectively.

Our study provides direct evidence that space-based lidar layer detection at 1064 nm is more representative of the true ACA scene compared to 532 nm. More importantly, our study suggests that the occurrence of aerosol entrainment into clouds might be much more frequent than previously thought based on CALIOP 532nm observations. This implies that the microphysical indirect effects could be an important mechanism through which the transported aerosol influences the clouds and radiation in SE Atlantic region. Finally, an accurate measurement of the vertical distribution of aerosols would also help us better understand the semi-direct effects of the smoke aerosols.

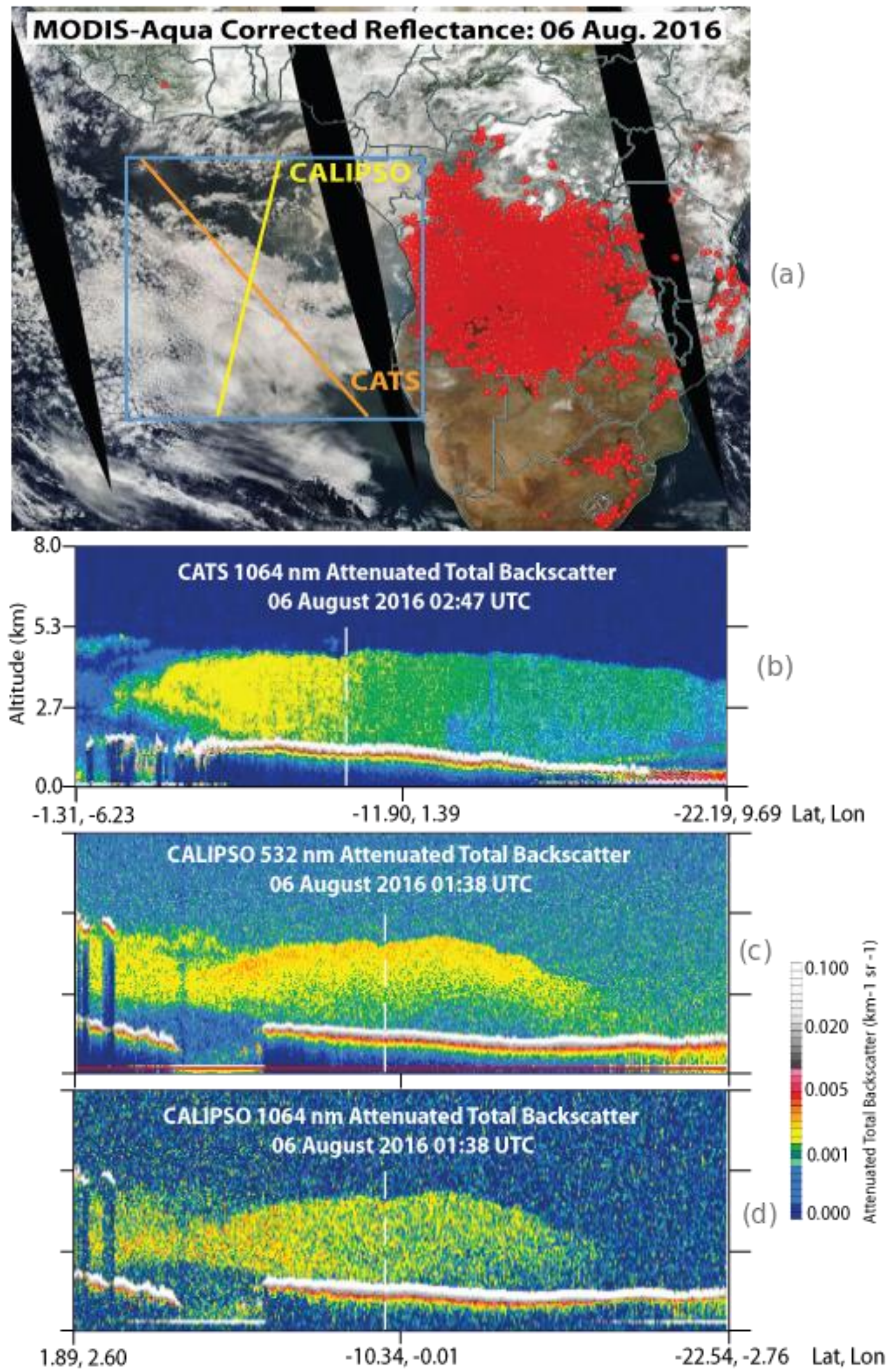

Figure 1 (a) A smoke above MBL cloud event on Aug. 06, 2016. Red dots in the African Continent are fire events. Attenuated total backscatter of CATS 1064nm (b), CALIPSO 532nm (c) and CALIPSO 1064nm. The dashed lines correspond to the point where the CAT and CALIPSO tracks overlap with each other.

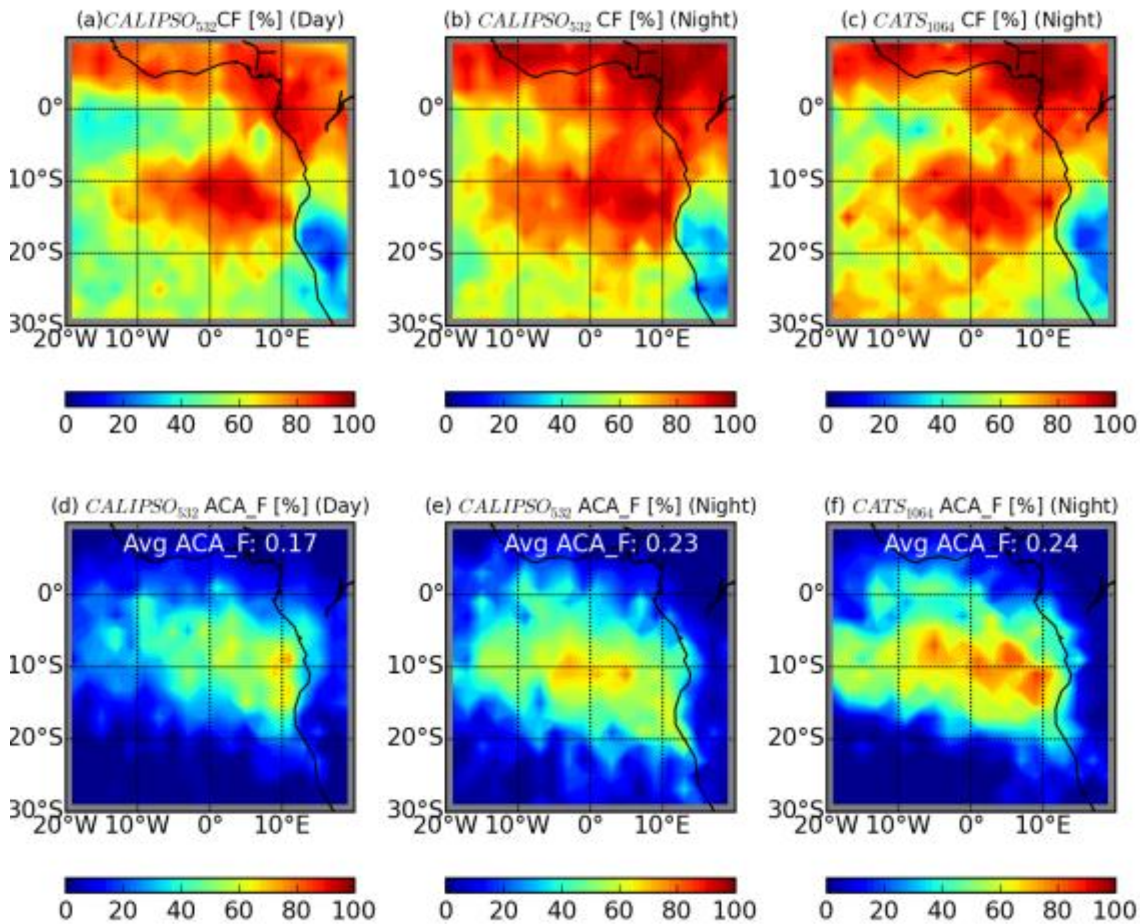

Figure 2 Multi-year (2015-2016) seasonal mean (July to October) cloud fraction (upper row) in the SE Atlantic region based on (a) CALIPSO daytime, (b) CALIPSO nighttime and (c) CATS nighttime observation. The seasonal mean occurrence frequency (lower row) from (d) CALIPSO daytime, (e) CALIPSO nighttime and (f) CATS nighttime observations.

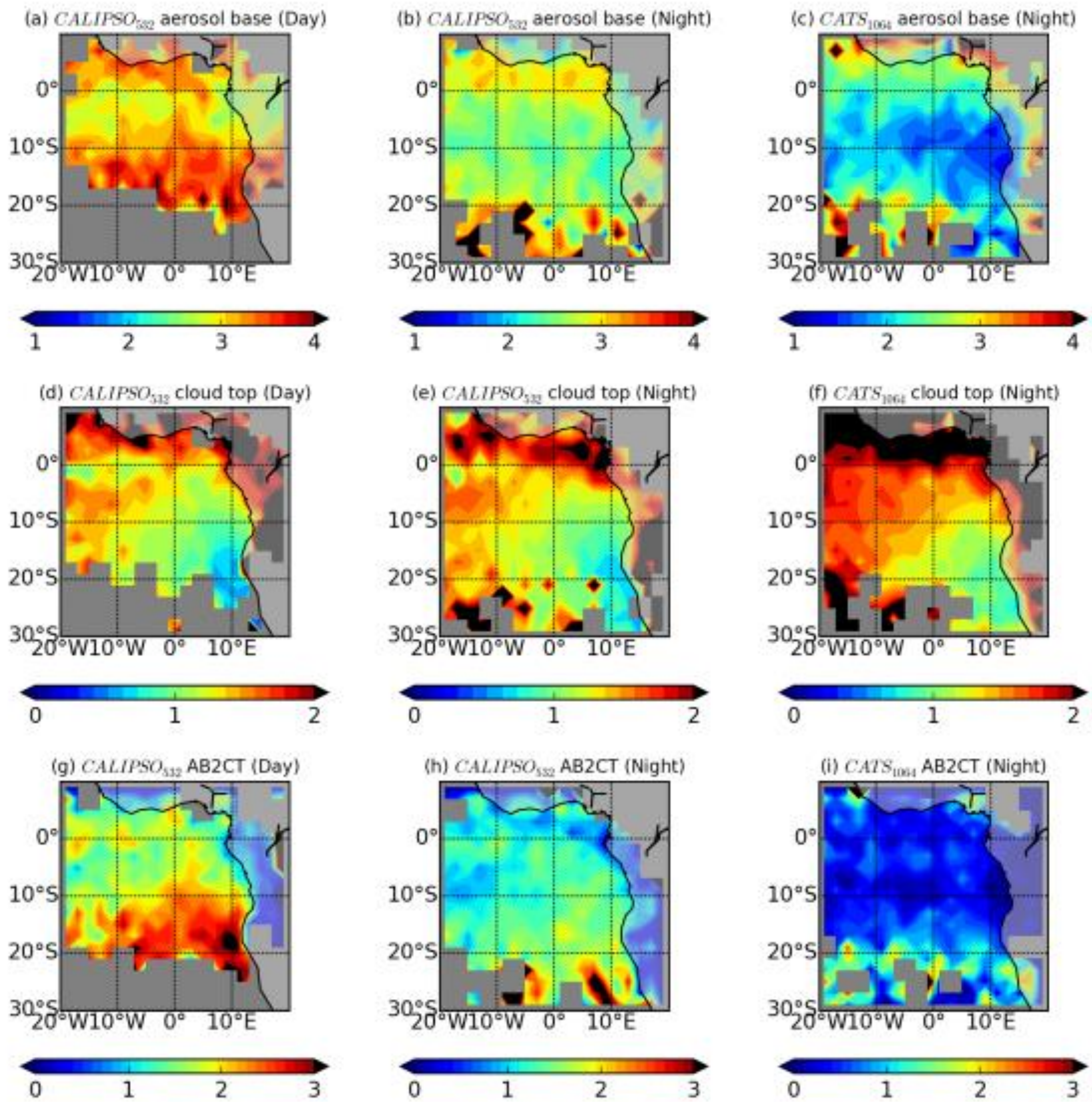

Figure 3 Multi-year (2015-2016) seasonal mean aerosol layer base height (top row), cloud layer top height (middle row), and aerosol base to cloud top (AB2CT) distance (bottom row) of ACA over the SE Atlantic region during JASO from CALIOP and CATS.

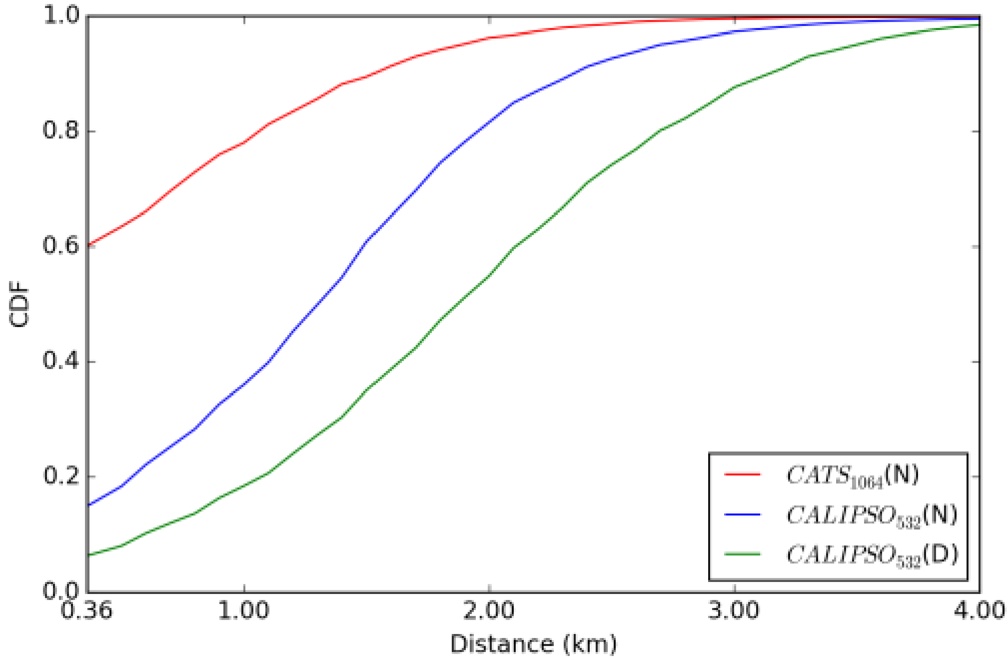

Figure 4 Cumulative probability distribution function of the distance between aerosol layer bottom and cloud top (AB2CT distance). These curves are derived from the multi-year seasonal ACA data used in Figure 3.

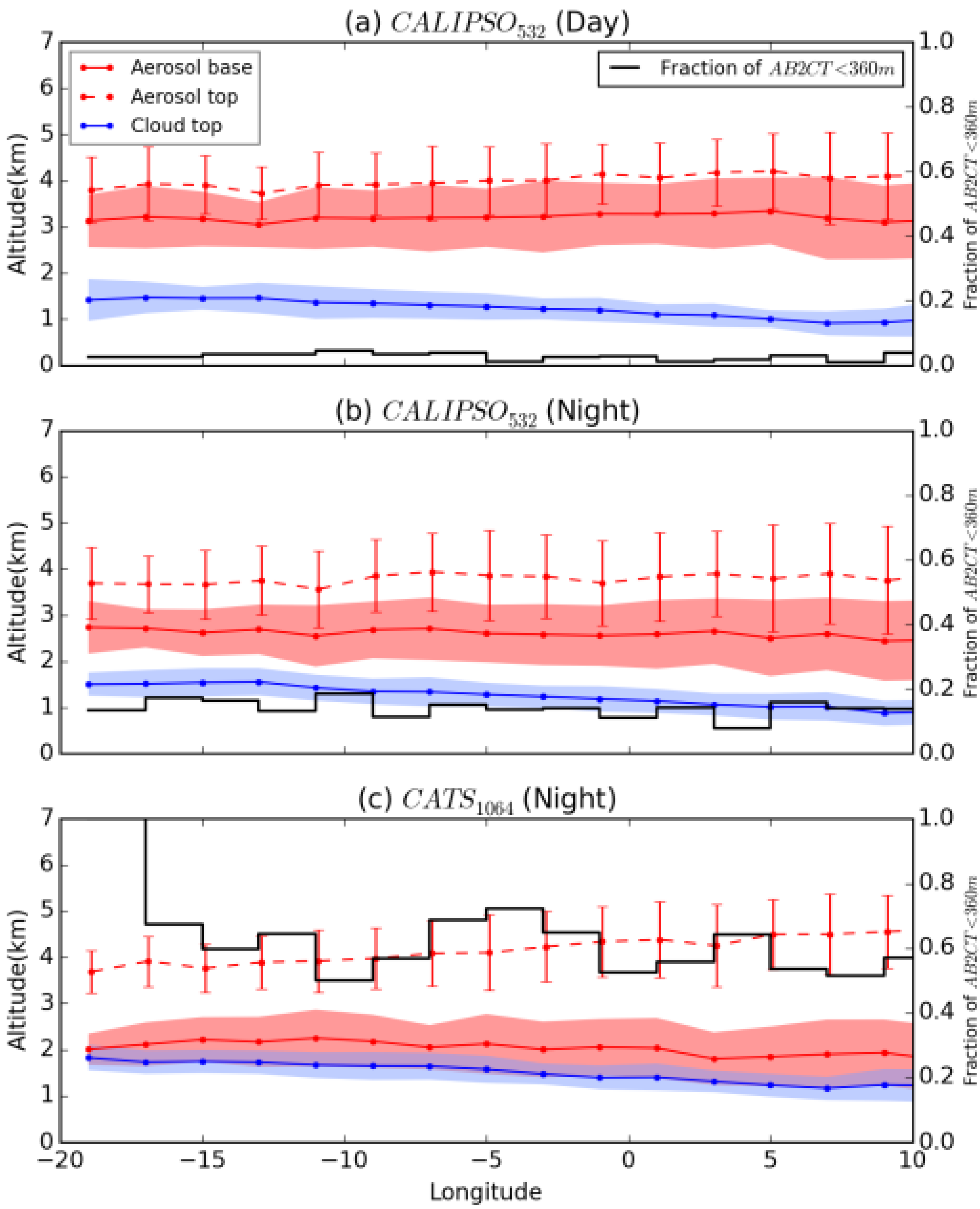

Figure 5 Meridionally-averaged aerosol bottom (solid red line), top (dashed red line) and cloud top (solid blue line) heights, with fraction of AB2CT<360m (black line), for the SE Atlantic region during JASO, 2015-2016. One standard deviation variability for each are denoted by the red error bars for aerosol top height, and by the red and blue shaded regions for the aerosol bottom and cloud top heights, respectively.

References

Adebiyi, A. A., and P. Zuidema (2016), The role of the southern African easterly jet in modifying the southeast Atlantic aerosol and cloud environments, *Quarterly Journal of the Royal Meteorological Society*, *142*(697), 1574–1589, doi:10.1002/qj.2765.

Burton, S. P., R. A. Ferrare, M. A. Vaughan, A. H. Omar, R. R. Rogers, C. A. Hostetler, and J. W. Hair (2013), Aerosol classification from airborne HSRL and comparisons with the CALIPSO vertical feature mask, *Atmos. Meas. Tech.*, *6*(5), 1397–1412, doi:10.5194/amt-6-1397-2013.

Chand, D., R. Wood, T. L. Anderson, S. K. Satheesh, and R. J. Charlson (2009), Satellite-derived direct radiative effect of aerosols dependent on cloud cover, *Nature Geoscience*, *2*(3), 181–184, doi:10.1038/ngeo437.

Chand, D., T. L. Anderson, R. Wood, R. J. Charlson, Y. Hu, Z. Liu, and M. Vaughan (2008), Quantifying above‐cloud aerosol using spaceborne lidar for improved understanding of cloudy‐sky direct climate forcing, *J. Geophys. Res.*, *113*(D13), D13206, doi:10.1029/2007JD009433.

Costantino, L., and F. M. Bréon (2013), Aerosol indirect effect on warm clouds over South-East Atlantic, from co-located MODIS and CALIPSO observations, *Atmospheric Chemistry and Physics*, *13*(1), 69–88, doi:10.5194/acp-13-69-2013.

Costantino, L., and F.-M. Bréon (2010), Analysis of aerosol-cloud interaction from multi-sensor satellite observations, *Geophysical Research Letters*, *37*(11), L11801–n/a, doi:doi:10.1029/2009GL041828.

Devasthale, A., and M. A. Thomas (2011), A global survey of aerosol-liquid water cloud overlap based on four years of CALIPSO-CALIOP data, *Atmospheric Chemistry and Physics*, *11*(3), 1143–1154, doi:10.5194/acp-11-1143-2011.

Hu, Y., M. Vaughan, Zhaoyan Liu, K. Powell, and S. Rodier (2007), Retrieving Optical Depths and Lidar Ratios for Transparent Layers Above Opaque Water Clouds From CALIPSO Lidar Measurements, *Geoscience and Remote Sensing Letters, IEEE DOI - 10.1109/LGRS.2007.901085*, *4*(4), 523–526.

Jethva, H., O. Torres, F. Waquet, D. Chand, and Y. Hu (2014), How do A‐train sensors intercompare in the retrieval of above‐cloud aerosol optical depth? A case study‐based assessment, *Geophysical Research Letters*, *41*(1), 186–192, doi:10.1002/2013GL058405.

Johnson, B. T., K. P. Shine, and P. M. Forster (2004), The semi-direct aerosol effect: Impact of absorbing aerosols on marine stratocumulus, *Quarterly Journal of the Royal Meteorological Society*, *130*(599), 1407–1422, doi:10.1256/qj.03.61.

Kacenelenbogen, M., M. A. Vaughan, J. Redemann, R. M. Hoff, R. R. Rogers, R. A. Ferrare, P. B. Russell, C. A. Hostetler, J. W. Hair, and B. N. Holben (2011), An accuracy assessment of the CALIOP/CALIPSO version 2/version 3 daytime aerosol extinction product based on a detailed multi-sensor, multi-platform case study, *Atmospheric Chemistry and Physics*, doi:10.5194/acp-11-3981-2011.

Liu, Z., D. Winker, A. Omar, M. Vaughan, J. Kar, C. Trepte, Y. Hu, and G. Schuster (2015), Evaluation of CALIOP 532 nm aerosol optical depth over opaque water clouds, *ACP*, *15*(3), 1265–1288, doi:10.5194/acpd-14-23583-2014.

Liu, Z., M. A. Vaughan, D. M. Winker, C. A. Hostetler, L. R. Poole, D. Hlavka, W. Hart, and M. McGill (2004), Use of probability distribution functions for discriminating between cloud and aerosol in lidar backscatter data, *J. Geophys. Res.*, *109*(D15), 1275, doi:10.1029/2004JD004732.

Liu, Z., M. Vaughan, D. Winker, C. Kittaka, B. Getzewich, R. Kuehn, A. Omar, K. Powell, C. Trepte, and C. Hostetler (2009), The CALIPSOLidar Cloud and Aerosol Discrimination: Version 2 Algorithm and Initial Assessment of Performance,, *26*(7), 1198–1213, doi:10.1175/2009JTECHA1229.1.

McGill, M. J., J. E. Yorks, V. S. Scott, A. W. Kupchock, and P. A. Selmer (2015), The Cloud-Aerosol Transport System (CATS): a technology demonstration on the International Space Station, edited by U. N. Singh, *SPIE Optical Engineering + Applications*, *9612*, 96120A–96120A–6.

McGill, M. J., M. A. Vaughan, C. R. Trepte, W. D. Hart, D. L. Hlavka, D. M. Winker, and R. Kuehn (2007), Airborne validation of spatial properties measured by the CALIPSO lidar, *J. Geophys. Res.*, *112*(D20), 5522, doi:10.1029/2007JD008768.

Meyer, K., S. Platnick, and Z. Zhang (2015), Simultaneously inferring above‐cloud absorbing aerosol optical thickness and underlying liquid phase cloud optical and microphysical properties using MODIS, *Journal of Geophysical Research-Atmospheres*, *120*(11), 5524–5547, doi:10.1002/2015JD023128.

Meyer, K., S. Platnick, L. Oreopoulos, and D. Lee (2013), Estimating the direct radiative effect of absorbing aerosols overlying marine boundary layer clouds in the southeast Atlantic using MODIS and CALIOP, *Journal of Geophysical Research-Atmospheres*, *118*(10), 4801–4815, doi:10.1002/jgrd.50449.

Min, M., and Z. Zhang (2014), On the influence of cloud fraction diurnal cycle and sub-grid cloud optical thickness variability on all-sky direct aerosol radiative forcing, *Journal of Quantitative Spectroscopy and Radiative Transfer*, *142 IS -*, 25–36, doi:10.1016/j.jqsrt.2014.03.014.

Painemal, D., P. Minnis, and M. Nordeen (2015), Aerosol variability, synoptic‐scale processes, and their link to the cloud microphysics over the northeast Pacific during MAGIC, *Journal of Geophysical Research-Atmospheres*, *120*(10), 5122–5139, doi:10.1002/2015JD023175.

Sakaeda, N., R. Wood, and P. J. Rasch (2011), Direct and semidirect aerosol effects of southern African biomass burning aerosol, *J Geophys Res*, *116*(D12), D12205, doi:10.1029/2010JD015540.

Torres, O., C. Ahn, and Z. Chen (2013), Improvements to the OMI near-UV aerosol algorithm using A-train CALIOP and AIRS observations, *Atmos. Meas. Tech.*, *6*(11), 3257–3270, doi:10.5194/amt-6-3257-2013.

Torres, O., H. Jethva, and P. K. Bhartia (2011), Retrieval of Aerosol Optical Depth above Clouds from OMI Observations: Sensitivity Analysis and Case Studies, *J. Atmos. Sci.*, *69*(3), 1037–1053, doi:10.1175/JAS-D-11-0130.1.

Vaughan, M. A., K. A. Powell, D. M. Winker, C. A. Hostetler, R. E. Kuehn, W. H. Hunt, B. J. Getzewich, S. A. Young, Z. Liu, and M. J. McGill (2009), Fully Automated Detection of Cloud and Aerosol Layers in the CALIPSO Lidar Measurements, *J. Atmos. Oceanic Technol.*, *26*(10), 2034–2050, doi:doi: 10.1175/2009JTECHA1228.1.

Waquet, F., J. Riedi, L. C Labonnote, P. Goloub, B. Cairns, J. L. Deuzé, and D. Tanre (2009), Aerosol Remote Sensing over Clouds Using A-Train Observations, *J. Atmos. Sci.*, *66*(8), 2468–2480, doi:10.1175/2009JAS3026.1.

Wilcox, E. M. (2010), Stratocumulus cloud thickening beneath layers of absorbing smoke aerosol, *Atmospheric Chemistry and Physics*, *10*(23), 11769–11777, doi:10.5194/acp-10-11769-2010.

Wilcox, E. M. (2012), Direct and semi-direct radiative forcing of smoke aerosols over clouds, *Atmospheric Chemistry and Physics*, *12*(1), 139–149, doi:10.5194/acp-12-139-2012.

Winker, D. M., M. A. Vaughan, A. Omar, Y. Hu, K. A. Powell, Z. Liu, W. H. Hunt, and S. A. Young (2009), Overview of the CALIPSO mission and CALIOP data processing algorithms,, *26*(11), 2310–2323.

Yorks, J. E., D. L. Hlavka, M. A. Vaughan, M. J. McGill, W. D. Hart, S. Rodier, and R. Kuehn (2011), Airborne validation of cirrus cloud properties derived from CALIPSO lidar measurements: Spatial properties, *J. Geophys. Res.*, *116*(D19), 1073, doi:10.1029/2011JD015942.

Yorks, J. E., M. J. McGill, S. P. Palm, D. L. Hlavka, P. A. Selmer, E. P. Nowottnick, M. A. Vaughan, and S. D. Rodier (2015), An Overview of the Cloud-Aerosol Transport System (CATS) Processing Algorithms and Data Products.

Yorks, J. E., M. J. McGill, S. P. Palm, D. L. Hlavka, P. A. Selmer, E. P. Nowottnick, M. A. Vaughan, S. D. Rodier, and W. D. Hart (2016), An overview of the CATS level 1 processing algorithms and data products, *Geophysical Research Letters*, *43*(9), 4632–4639.

Yu, H., and Z. Zhang (2013), New Directions: Emerging satellite observations of above-cloud aerosols and direct radiative forcing, *Atmospheric Environment*, *72*(0), 36–40, doi:10.1016/j.atmosenv.2013.02.017.

Yu, H., Y. Zhang, M. Chin, Z. Liu, A. Omar, L. A. Remer, Y. Yang, T. Yuan, and J. Zhang (2010), An integrated analysis of aerosol above clouds from A-Train multi-sensor measurements, *Remote Sensing of Environment*, *121*, 125–131, doi:10.1016/j.rse.2012.01.011.

Zhang, Z., K. Meyer, H. Yu, S. Platnick, P. Colarco, Z. Liu, and L. Oreopoulos (2016), Shortwave direct radiative effects of above-cloud aerosols over global oceans derived from 8 years of CALIOP and MODIS observations, *ACP*, *16*(5), 2877–2900, doi:10.5194/acpd-15-26357-2015.